Research Article

Journal of PeptideScience

Received: 22 April 2010 Revised: 30 August 2010 Accepted: 10 September 2010 Published online in Wiley Online Library: 23 November 2010

(wileyonlinelibrary.com) DOI 10.1002/psc.1311

The action of fish peptide Orpotrin analogs on microcirculation

Katia Conceição,[a] Fernanda Miriane Bruni,[a] Juliane M. Santos,[b] Robson Melo Lopes,[a] Elineide E. Marques,[b] Jorge H. Fernandez[c] and Mônica Lopes-Ferreira[a]*

In order to investigate the relationship between the primary structure of Orpotrin, a vasoactive peptide previously isolated from the freshwater stingray *Potamotrygon gr. orbignyi*, and its microcirculatory effects, three Orpotrin analogs were synthesized. The analogs have a truncated *N*-terminal with a His residue deletion and two substituted amino acid residues, where one Nle is substituted for one internal Lys residue and the third analog has a substitution of a Pro for an Ala (Orp-desH[1], Orp-Nle and Orp-Pro/Ala, respectively). Only Orp-desH[1] could induce a lower vasoconstriction effect compared with the natural Orpotrin, indicating that besides the *N*-terminal, the positive charge of Lys and the Pro residues located at the center of the amino acid chain is crucial for this vasoconstriction effect. Importantly, the suggestions made with bioactive peptides were based on the molecular modeling and dynamics of peptides, the presence of key amino acids and shared activity in microcirculation, characterized by intravital microscopy. Moreover, this study has demonstrated that even subtle changes in the primary structure of Orpotrin alter the biological effects of this native peptide significantly, which could be of interest for biotechnological applications. Copyright © 2010 European Peptide Society and John Wiley & Sons, Ltd.

Supporting information may be found in the online version of this article

Keywords: Orpotrin; *Potamotrygon* stingrays; vasoactivity; microcirculation

Introduction

The search for lead compounds for the development of new therapeutic agents has long included a focus on animal venoms. This is primarily because venomous animals have evolved complex mixtures of biologically active compounds and toxins that target vital physiological processes in their prey and, inadvertently, often in humans. Most animal toxins are highly selective and potent, qualities that often make them ideal lead compounds. Many animal venoms, including those from spiders, snakes, cone snails, scorpions and others, contain components that target the transmission of nerve impulses (i.e. neurotoxins) because this results in rapid immobilization or death of the animal's prey [1]. However, there are also many other venom components that have profound effects on the cardiovascular system [2].

Fish tissues and organs are a rich source of these biologically active compounds involved in both the regulation of physiological functions and the defense against predators or microorganisms. In particular, the study on the occurrence of bioactive peptides in fish species, undertaken in the early 1960s, led to the discovery of a number of peptides with different pharmacological activities, such as vasotocin [3], insulin [4] and an increasing number of antimicrobial peptides isolated including cathelicidins [5], epinecidin [6], misgurin [7], pardaxins [8] and piscidins [9].

Venom peptide seems to have evolved from a relatively small number of structural frameworks that are particularly well suited to addressing the crucial issues of potency and stability. A few of the peptides isolated from venomous fish include the pardaxins from *Pardachirus* species [10,11], hepcidins from channel catfish *Ictalurus punctatus* [12], one ghrelin-like peptide isolated from the stomach of *Dasyatis akajei* stingray [13] and the two peptides Orpotrin and Porflan from the venom of *Potamotrygon gr orbignyi*, isolated by our group [14,15]. The last two peptides were active in mice cremaster microcirculation, inducing vasoconstriction and inflammation, respectively.

Orpotrin is a short, linear vasoconstrictor peptide consisting of nine amino acid residues, *His-Gly-Gly-Tyr-Lys-Pro-Thr-Asp-Lys*; because of its sequence alignment with creatine kinase (CK) residues 97–105 (. . .LL^{90}DPVIQDR**HGGYKPTDK**HKTDL^{110}NP. . .) localized between two basic residues, Arg96 and Lys105, the generation of Orpotrin could be associated to the limited proteolysis product of CK, in the same way as the other well-characterized bioactive peptides such as Hemorphins [16] and Parasin I [17,18].

Although many natural and venom peptides have been described, there is a great potential for the development of

* *Correspondence to: Mônica Lopes-Ferreira, Avenida Vital Brazil 1500, São Paulo – SP, 05503-900, Brazil. E-mail: lopesferreira@butantan.gov.br*

a *LETA (Laboratório Especial de Toxinologia Aplicada) Center for Applied Toxinology (CAT/CEPID), Butantan Institute, São Paulo, SP, Brazil*

b *Nucleus of Environmental Studies, Federal Univesity of Tocantins, Tocantins, Brazil*

c *LQFPP-CBB – Universidade Estadual do Norte Fluminense – UENF, Campo dos Goytacazes, Rio de Janeiro, Brazil*

Journal of PeptideScience

synthetic analogs based on existing structures and with increased specific activity [19]. Several works described the design, synthesis, structural analysis and activity of analogs of peptide toxins that are intended to mimic the native toxin [15,20,21]. In our previous paper describing Orpotrin, the microcirculatory environment was our biological target. Topical application of Orpotrin in mice cremaster muscle exerted significantly stronger vasoconstrictive effects on large arterioles [14].

The vascular endothelium is a complex and dynamic organ and one of the largest secretory tissues of mammals [22,23]. The vascular endothelium, once thought to be only a mechanical barrier between the blood and the vessel wall, is now recognized to be an endocrine organ showing an amazing variety of regulatory functions. Endothelium-derived mediators have essential functions in vascular regulation [23]. Endothelial dysfunction involves an imbalance between vasoregulating substances together with a disturbance of hemostasis and vessel structure, resulting in the development of cardiovascular diseases, such as hypertension, atherosclerosis and heart failure. It is accepted that vasoconstrictive substances generally play a central role in the physiology and pathology of vascular regulation. They also mediate vascular tone; structure and function; and influence vascular smooth muscle cell (VSMC) proliferation, apoptosis [24], platelet aggregation [25], monocyte and leukocyte adhesion [26] as well as thrombosis [27].

The endothelial functionality of microcirculation often reflects the status of the entire vascular system, and changes in its regulation often appear in early stages of a disease, not seldom before any effects on the systemic regulation are noticed [28,29]. However, such changes may be difficult to assess, and it may be stated that few, if any, techniques are used clinically today for this purpose. Intravital microscopy is one of the reliable techniques that can be used *in vivo* for accurate assessment of the microvascular environment and may be used to better understand the underlying mechanisms of vasoactive substances [30]. Taking into account this background, the aims of this work are (i) to identify the mutation(s) that support the Orpotrin vasoconstrictor activity through the synthesis of three Orpotrin analogs and testing their role in microcirculation and (ii) to investigate the impact of these amino acid changes on structural stability, and physicochemical characteristics and/or the effects on the vasoconstrictor activity based on the structure of toxins and vasoactive peptides. The relationship obtained between structural features and biological activity, in terms of the microcirculation, is discussed.

Material and Methods

Molecular Modeling and Structure Dynamics of Orpotrin Analogs

Besides the naturally occurring peptide Orpotrin, three analogs were chosen for the structure–activity relationship studies, Orp-Nle (H G G Y Nle P T D K), Orp-desH[1] (G G Y K P T D K) and Orp-Pro/Ala (H G G Y K A T D K).

Orpotrin and analogs were modeled using ChemDraw Ultra 8.0 (CambridgeSoft, Cambridge, USA) and the initial three-dimensional structure was obtained using Chem3D Ultra 8.0 (CambridgeSoft, Cambridge, USA). Standard protonation at pH 7.0 was implemented in the structures obtained using extended Hûckel Charges, and energy minimization was implemented using the PM6 semi-empirical quantum chemistry method [31] in MOPAC2009 (http : OpenMOPAC.net). To access additional information in structural dynamics of Orpotrin analogs, additional energy minimization and equilibrating molecular dynamics simulations were carried out with the Gromacs 4.02 package [32] on a dual-QuadCore Linux workstation using the GROMOS96 53a5 [33] force field and representing more than 10 000 h/CPU computational work and 12 Gb of data mining. Initial structures were subjected to a steepest decent (SD) energy minimization (5000 steeps) in an SPC water box to remove bad van der Waals contacts. For further relaxation, minimized structures of solvation box were used in unrestrained molecular dynamics for 10 ns with Berendsen-type temperature (310 K) and pressure (1 atm.) coupling in an NPT simulation cell, implementing the PME method of electrostatic treatment [34]. Production dynamics were the same as for 350–390 ns. Cluster analysis of the obtained trajectory was performed using the g_cluster program of Gromacs 4.02 [32] whit 2.0 Å cutoff. Diagonalization of 2400 × 24 001 obtained matrixes was used to analyze representative structures of the analogs during production simulation. The structures of the five most representative clusters in the molecular dynamics run were selected for further analysis of peptide conformational space.

Peptide Synthesis

Orpotrin and analogs were synthesized by solid-phase peptide synthesis on an Fmoc-Lys(Boc)-NovaSyn® TGA (Novabiochem, Nottingham, UK) by using the Fmoc strategy in an automated bench-top simultaneous multiple solid-phase synthesizer (PSSM 8 system from Shimadzu Co.) [35]. Couplings were performed with *o*-(Benzotriazol-1-yl)-*N*,*N*,*N*′,*N*′-tetramethyluronium tetrafluoroborate (TBTU)/1-hydroxybenzotriazole in *N*,*N*-dimethylformamide for 60 min. The synthesized peptides were cleaved from the resin by the addition of TFA/thioanisole/1,2-ethanedithiol/phenol/water solution (82.5 : 5 : 2.5 : 5 : 5) at room temperature for 8 h. The peptide products removed from the resin were diluted in water/acetonitrile (9 : 1) and lyophilized.

Synthetic peptides were purified by RP-HPLC (Shimadzu LC10 VP Series, Kyoto, Japan) using a semi-preparative Shimadzu C18 column (Shim-pack Prep-ODS, 5 µm, 20 × 250 mm). A gradient of 5–45% of acetonitrile containing 0.1% TFA (solvent B) in 35 min was applied, where solvent A was ultra-pure H_2O containing 0.1% TFA. The purified fractions containing the peptide were pooled and lyophilized.

Mass Spectrometry

Molecular mass analyses of the purified peptides were performed on a MALDI-TOF MS in an Ettan MALDI-TOF/Pro system (Amersham Biosciences, Uppsala, Sweden) in reflectron mode calibrated with P14R ($[M+H]^+$ 1533.8582) and angiotensin II ($[M+H]^+$ 1046.5423) (Sigma). MALDI-TOF spectra were obtained in the positive ion mode at an acceleration voltage of 20 kV. The matrix solution used contained saturated α-cyano-4-hydroxycinnamic acid (Sigma) in 50% acetonitrile/0.1% TFA.

Biological Investigation

Animals

Groups of four Swiss mice weighing 18–22 g were used throughout. The animals provided by Instituto Butantan animal house were kept in temperature- and humidity-controlled rooms and received food and water *ad libitum*. The local ethical committee (CEUAIB/Butantan Institute) approved the experiments involving mice.

Intravital microscopy

The dynamics of alterations in the microcirculatory network were determined using intravital microscopy by transillumination of the mice cremaster muscle after topical application of the investigated peptides (500 nM/kg) dissolved in 20 µl of sterile saline solution. Administration of the same amount of sterile saline (20 µl) was used as a control. Before beginning the experiments, mice were injected with a muscle relaxant drug (0.4% Xilazin) (Coopazine®, Schering-Plough Coopers Brasil Ltda., São Paulo, Brasil) and then anesthetized with 0.2 g/kg chloral hydrate, and the cremaster muscle was exposed for microscopic examination *in situ* as previously described [36,37]. The animals were maintained on a specially designed board controlled thermostatically at 37 °C, which included a transparent platform on which the transilluminated tissue was placed.

The study of the microvascular system of transilluminated tissue was performed using an optical microscope (Axiolab, Carl Zeiss, Oberkochen, Germany) coupled to a photographic camera (AxioCam ICc1, Carl Zeiss, Oberkochen, Germany) using a 10/0.25 longitudinal distance objective/numeric aperture and 1.6 optovar (Carl Zeiss, Oberkochen, Germany) using a 10/0.3 longitudinal distance objective/numeric aperture and 1.6 optovar. All of the determinations mentioned were performed in triplicate.

Leukocyte recruitment measurements

After stabilization of the microcirculation, the number of rolling and adherent leukocytes in the postcapillary venules was counted 10 min after peptide topical application. A leukocyte was considered to be adhering to the venular endothelium if it remained stationary for 60 s or longer at a preset distance of 100 µm. A rolling leukocyte was defined as a white cell that moved slower than the stream of flowing erythrocytes. The number of rolling leukocytes was quantified as the number of white cells that passed a preset fixed point.

Arteriolar diameter measurements

Before topical application of the peptides, we scanned the selected arterioles (30–40 µm) and recorded their control diameters. We selected a vessel where both walls could be clearly visualized and were not obscured by overlying vessels. Once preliminary control values were recorded, we applied the peptides (10 nM) topically. We recorded the arterioles with 5 min intervals and measured the diameter. To compare the diameters, we considered the first record as time zero, being the percentage where no alterations were seen (baseline).

Statistical Analysis

All results are expressed as mean + SEM. One Way Analysis of Variance (ANOVA) followed by Dunnett's test was used to determine the levels of difference between all groups. Differences were considered statistically significant at $p < 0.05$.

Results

Orpotrin and Analogs '*In Silico*' Structural Analysis

In order to elucidate the structure–activity relationship of Orpotrin, molecular modeling in ChemDraw and Chen3D was used to assess the structural and physicochemical characteristics of the peptide. Also, the contribution of changes in Lys 5 (Orp-Nle analog), Pro 7 (Orp-Pro/Ala analog) and His 1 (Orp-desH[1] analog) to the characteristics described above and structure dynamics were analyzed in Figure S1 (see Supporting Information). Table 1 presents Orpotrin and the analogs that were synthesized, analyzed by RP-HPLC and MALDI MS.

Table 1. Molecular mass (Da) of the natural and analogs of Orpotrin

Peptides	Sequence	Molecular mass (Observed)[a]	Molecular mass (Theoretical)	Retention time (min)[b]
Orpotrin	**H** G G Y **K P** T D K	1002.046	1002.500	5.1
Orp-Nle	H G G Y **Nl** P T D K	987.536	987.489	12.1
Orp-desH[1]	G G Y K P T D K	865.446	865.441	9.5
Orp-Pro/Ala	H G G Y K **A** T D K	976.516	976.486	8.9

[a] Observed by MALDI-TOF/MS.
[b] Analytical HPLC determinations were carried in 6 × 150 mm RP-C18 column, out two solvent systems: (A) 0.1% TFA in CH_3CN and (B) 0.1% TFA in H_2O; linear gradient from 5% (B) to up to 90% (B) over 25 min, UV detection at 220 nm, flow rate 1 ml/min.
Values in bold are the replaced amino acids.

After subsequent rounds of charges calculation using the semiempirical PM3 method [31] and energy minimization using MOPAC2009, the structure of Orpotrin obtained was very close to a small B-element with close *N*- and *C*-terminals. An important contribution of the electrostatic interactions between Asp8 *N*-terminal and Lys9 *C*-terminal was observed in Orpotrin and the Orp-Nle analog but the ones obtained in vacuo structures for Orp-desH[1] and Orp-Pro/Ala were different, but the overall changes in physicochemical properties were hard to analyze in these conditions as the final minimized structure of peptides was fully dependent on initial drawing in ChemDraw8 (Figure S1).

As charged groups and electrostatic potential can have an important role in the binding characteristics of the peptides, replacement of protonated Lys5 by Nle (Orp-Nle analog) mimics the situation where an aliphatic position is generated with no big impact in the structure. In addition, Pro6 was mutated to Ala (Orp-Pro/Ala), looking for potential implications in the conformation or dynamics at the center of the peptide structure. Finally, His provides an example of a polar, basic (positively charged) amino acid, and its removal must result in a more non-polar *N*-terminal site and small peptide structure (Figures 1(A), S1 and Table 1). Although no big differences in electrostatic potential or structural shape after energy minimization were detected in Orpotrin and analogs (Figure 1(B)), semi-empirical calculations using the PM6 model in MOPAC of these peptides revealed an increasing hydrophobicity in Orp-Nle analog if compared with the other peptides. The small Orp-desH[1] peptide was the most convergent in energy minimization analyses (data not shown).

For a better understanding of the impact of these structural changes in the dynamics of Orpotrin and analogs, 350 ns molecular simulations in explicit solvent were used to calculate the conformational space of each peptide. As the structure fluctuation of small peptides impacts on the recognition and binding capabilities, more stable or chaotic structures are implicated in important differences in binding affinities or targets. Dynamics trajectories obtained in Gromacs package were used for comparative cluster analysis of most represented structures in Orpotrin and analogs (see Figure 1(C) and Figure S1 (A–B) for cluster analysis matrix). Conformational space of Orp-desH[1]

Journal of PeptideScience

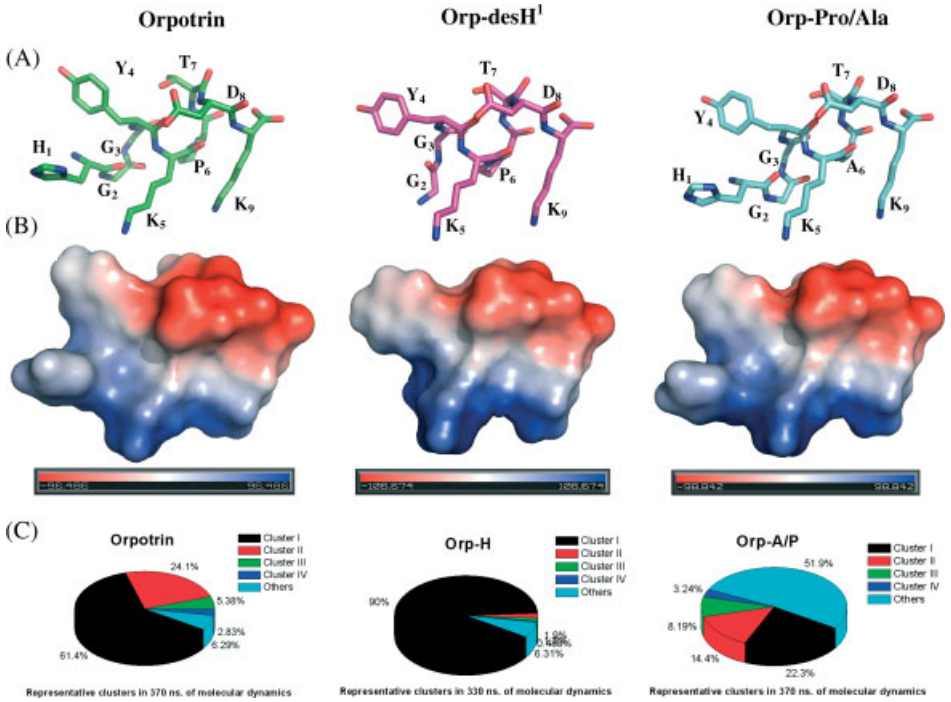

Figure 1. Physicochemical characteristics and structural dynamics of Orpotrin analogs. (A) Obtained initial structures for Orpotirn, Orp-desH[1] and Orp-Pro/Ala. (B) Electrostatic potential in the surface of the structures represented in color code (red for negative charges and blue for positive charges). (C) Analysis of representative structures in 360 ns of molecular simulation of Orpotrin analogs in water box. In all peptide structures and surfaces representations and rendering, Pymol 0.99 (www.pymol.org) was used.

was restricted to one structure in more than 90% of analyzed trajectories (Figure 1(C)), pointing to a more stable structure when compared with Orpotrin (61% of the conformational space occupied by the most represented structure). On the other hand, in Orp-Pro/Ala, the five most represented structures have only 49% of conformational space in 350 ns of simulation trajectory, indicating an increase in conformational entropy in peptide structure due to Pro6/Ala mutation (Figure 1(C)). In all analogs, the most represented structure was formed by a small central B-like element, with important electrostatic interactions between Asp8, Lys9 and *N*- and *C*-terminals (Figure S1(C)).

Orpotrin Analogs Effect in Arterioles

Swiss mice were used to access the effects of Orp-Nle, Orp-desH[1] and Orp-Pro/Ala at 10 nM (500 nM/kg) concentration on microcirculation environment. Figure 2 shows a representative time course of the changes in diameter of arterioles, with control diameters of about 45 μm, in response to the local application of Orpotrin analogs. As presented, the Orp-Nle did not induce a significant vasoconstrictor effect in arterioles. However, for Orp-desH[1] (Figure 2(C)), a decrease in the diameter of large arterioles was observed over the whole experimental duration and the maximal constriction occurred within 15 min (39.1%). The relative magnitude of arteriolar constriction in response to the Orp-desH[1] peptide was restored only partially after 30 min (15.7%).

Unlike the results observed for Orp-Nle and Orp-desH[1], the Orp-Pro/Ala analog presented a significant vasodilatation in arterioles (Figure 2(B)). A percentage increase in arteriolar diameter was observed over the whole experimental duration, as the highest response occurred at 15 min (26%).

In these experiments, observations were made on primary and secondary arterioles, but not on terminal arterioles. No change in diameter of venules was seen over time in either vehicle- or analog-treated animals.

Orpotrin Analogs Effect in Leukocytes

Topical application of the analogs and controls were carried out for up to 30 min (Figure 3(A)). A few rolling leukocytes were observed in the microcirculation of control mice (PBS bars). After the first 10 min of topical application of 10 nM of the synthetic Orp-Nle peptide, a significant increase in the number of rolling leukocytes in the post-capillary venule was induced, and this value was time dependent up to 40 min of the experimental period. Furthermore, the Orp-Nle analog promoted adhesion and transmigration of part of the leukocytes (Figure 3(B and C)) to the endothelial wall in the earliest times of the experiment. The analogs Orp-desH[1] and Orp-Pro/Ala at 10 nM did not affect significantly the number of rolling leukocytes, which remained at the basal values when compared to control.

Discussion

Initially, all replacements of residues in the Orpotrin amino acid chain does not cause radical variations in the global physicochemical proprieties of the peptides, as judged from molecular modeling and simulation experiment results (Figures 1 and S1). Given this fact, many of the suggestions were made regarding the changes in the primary structure of the peptide (Figure 1(C)).

Orpotrin analogs have been analyzed in the present study to assess the possible contributions of amino acid changes to vasoconstriction. When we analyzed the data, we were not surprised to find that substitution of Lys residues affects

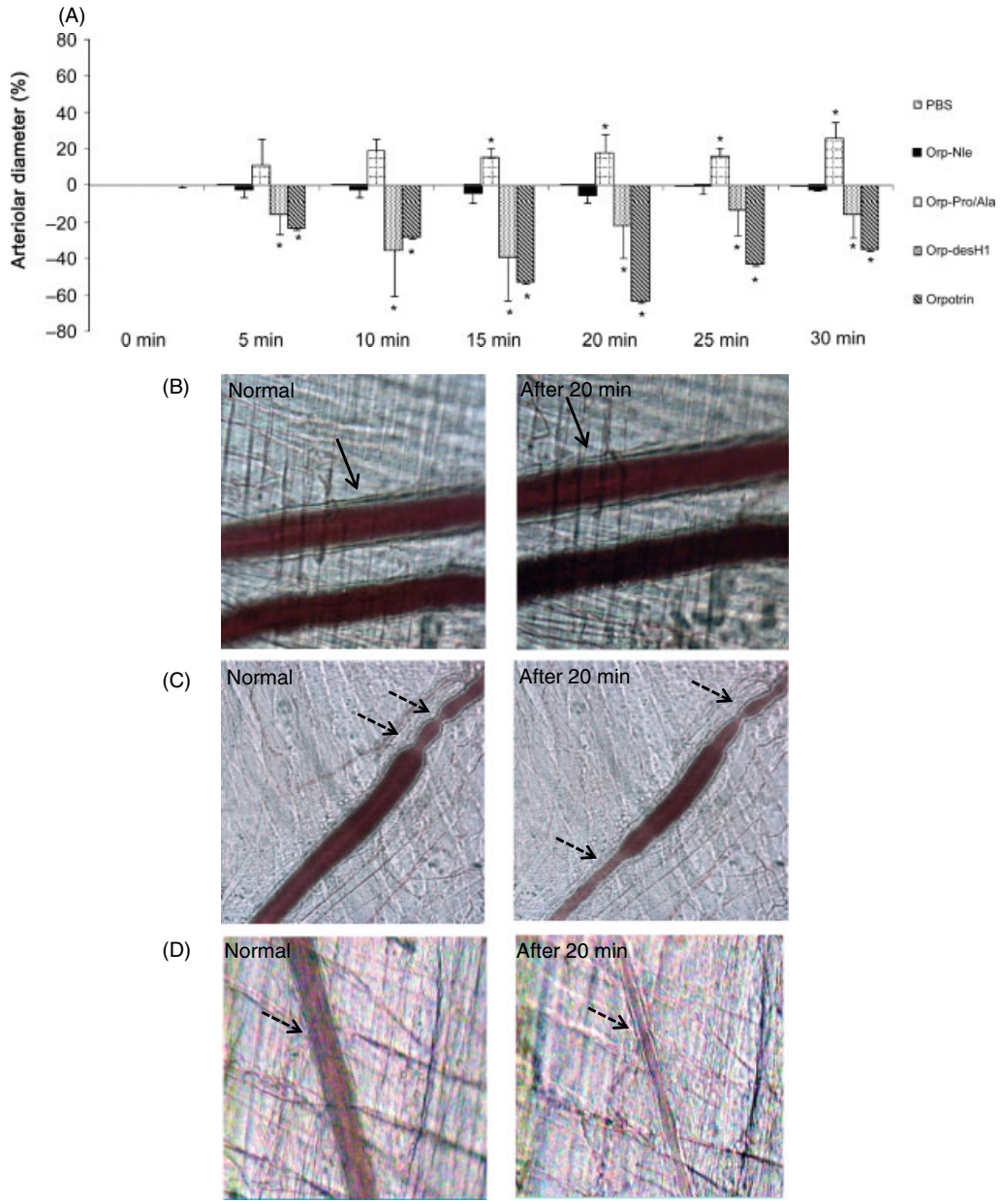

Figure 2. Intravital micrographs of cremaster muscle. (A) Representative graph showing arteriolar diameter percentage after topical application of 20 µl (10 nM) of Orpotrin analogs in different times. (B) Intravital micrograph of cremaster venule presenting arteriolar diameter increase after topical application of Orp-Pro/Ala. (C) Intravital micrograph of cremaster venule showing arteriolar diameter decrease after topical application of Orp-desH^1. (D) Intravital micrograph of cremaster venule showing arteriolar diameter decrease after topical application of Orpotrin. Photographs were obtained from digitized images on the computer monitor. Each point represents mean ± SEM. $^*p < 0.05$ compared with control group of three independent experiments.

vasoconstrictor activity, as it was already known from studies on numerous other molecules that cationic groups are necessary for this function [38,39]. Our results highlight the contextual or sequence-specific importance of Lys residues against a particular target. Replacing Lys for Nle (Orp-Nle), an *n*-butyl-group-substituted analog, abolishes the vasoconstrictor activity, indicating that Lys residue can contribute in a hydrophobic manner to the vasoconstrictor activity of Orpotrin through its methylene groups. Davies *et al*. [40] reported that the α-helical structure region containing three Lys residues in a linear fatty-acid-binding protein interacted with the anionic interface as a result of the initial electrostatic interaction [40]. Only these cationic residues contribute significantly to this binding. Other investigators suggest that apolipoprotein A-I Lys positive charges play an important role in the specific recognition of negatively charged phospholipids on the surface of a cell membrane transporter called the ATP-binding cassette transporter A-1, the ABCA1 [38].

Labarrère *et al*. [41] in a study with urotensin II, a cyclic vasoactive peptide initially isolated from the urophysis of the teleost fish *Gillichthys mirabilis*, shows that point substitution of Lys^8 in the urotensin II human analog totally suppresses the activity to contract rat thoracic aortic rings. These results support our data that the positively charged amino acid residue, i.e. Lys, is essential for binding activity on the peptide surface, and

Journal of PeptideScience

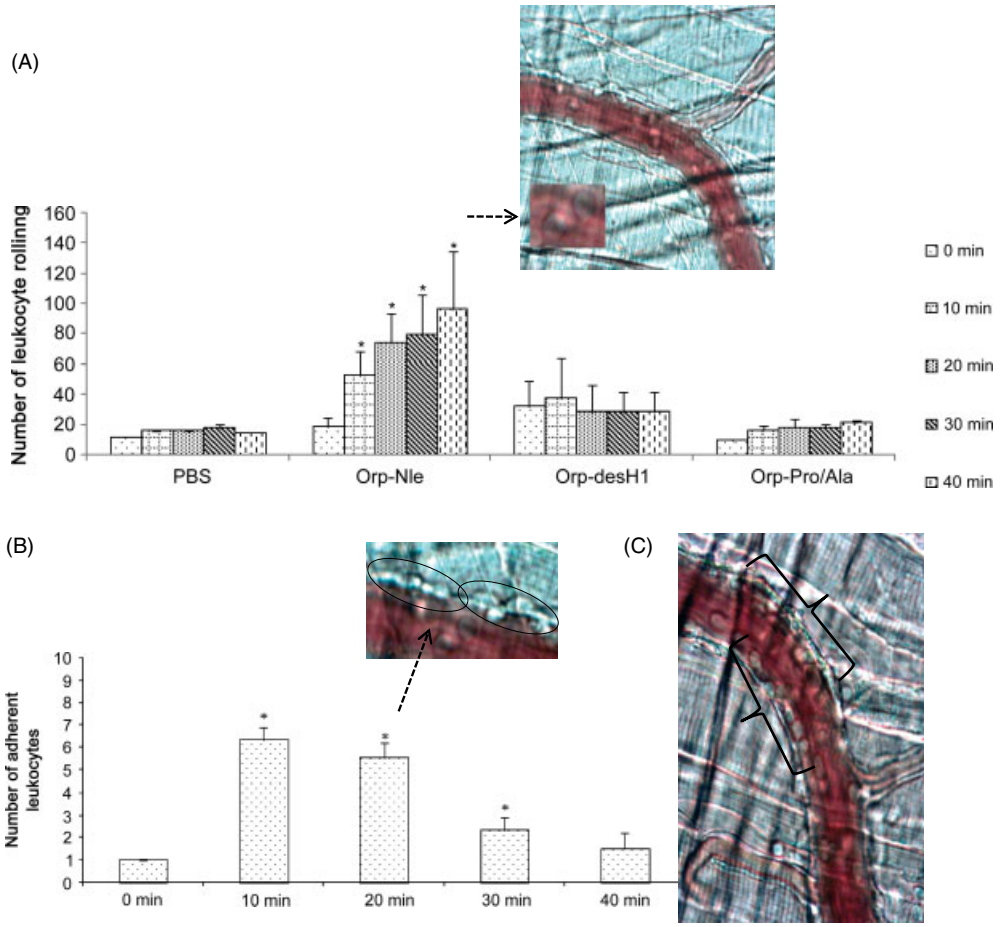

Figure 3. Intravital micrographs of cremaster muscle. (A) Representative graph showing leukocyte rolling of Orpotrin analogs in different times. Inset: Leukocyte rolling after 30 min of Orp-Nle administration (arrow). (B) Representative graph showing leukocyte adherent to endothelium after topical application of 20 µl (10 nM) of Orp-Nle. Inset: Leukocyte venular transmigration after 20 min of topical application. (C) Intravital micrograph of cremaster venule showing adherent leukocytes after Orp-Nle aplication. Photographs were obtained from digitized images on the computer monitor. Each point represents mean ± SEM. $^{*}p < 0.05$ compared with control group of three independent experiments.

may lead to stronger vasoconstriction observed for the Orpotrin peptide on microcirculation, whereas removal of the Lys amine group and retention of its hydrophobic *n*-butyl group improve an inflammatory activity.

For Orp-Pro/Ala analog the replacement has no effect in leukocyte recruitment (Figure 3(A)); however, an effect was observed in arterioles where this peptide caused a slight but significant increase in arteriolar diameter in large arterioles. The molecular mechanism of Pro stabilization in the case of vasoconstriction activity appears to be related to the fact that the pyrrolidine ring of Pro restricts the number of conformations that it can adopt compared with other residues (Figure 1(C)). Frare *et al*. [42], working with decorsin, a peptide isolated from the leech *Macrobdella decora*, suggest that Pro residues contribute to a significant and cumulative decrease in the high thermal stability observed in decorsin analogs with Pro→Ala substitutions. Meanwhile, Pro→Ala replacements can also produce context-dependent effects, since that in ubiquitin they had opposite effects in reducing or enhancing protein stability depending on the site of mutation along the protein chain [43]. The strategically important location of Pro^{6} suggests that even subtle alterations in the local environment of this region may dramatically influence the function of the peptide. The conformation at this location may be a necessary requirement to orient this peptide region toward the active site for the binding of receptors [44]. Increased flexibility in the Orp-Pro/Ala peptide, owing to the loss of Pro, is likely to impair this process and hence agonist interactions.

His residues are involved in substrate binding by many enzymes. The active His residue may act as a proton acceptor or donor in protein–ligand interactions, charge–relay interactions between amino acids at the active site, conformational changes associated with substrate binding or oligomerization of protein chains [45,46]. In Orp-$desH^{1}$, the removal of His^{1} caused at least 30% of decrease in vasoconstrictor activity (Figure 2) when compared with Orpotrin despite the apparent gain in structural stability (Figure 1(C)). Our results suggest that H^{1} makes modest contributions to the affinity binding site, triggering the vasoconstriction and characterizing a supporting role as a proton donor at the first residue for the conformational change of Orpotrin to form the receptor-binding region, or for an electrostatic interaction between Orpotrin and its receptor or protein.

As is well known, V1a-receptors located on vascular smooth muscle of arterioles mediate contraction and cause vasoconstriction [47], and thereby changes in arteriolar tone mainly contribute to the regulation of systemic vascular resistance and thus arterial blood pressure [48]. The combination of molecular modeling, synthesis of truncated peptides and site-directed mutagenesis [49–52] has shed light on hypothetical binding modes of AVP

or close analogs (oxytocin, vasotocin) to their specific receptors, although a clear consensus on the exact binding mode is still unknown. Rodrigo *et al*. [53] challenge the Arg8 residue of AVP and Lys8 analog with the two negatively charged residues (fully conserved in all V1a and V1b receptor) in close contact with Arg8 that were mutated to Ala in the human V1b receptor. As predicted, binding of AVP analogs to the mutant receptors was significantly decreased in both residues, for Lys this can be easily explained by its potential to develop ionic interactions with the two negatively charged residues. It is likely that the interaction predicted herein is a common feature of AVP recognition and it could also be a hypothesis for a possible candidate to orpotrin receptor recognition.

In summary, the three Orpotrin analogs were able to induce some bioactive function. Conversely, only Orp-desH^1, having a truncated *N*-terminal, could induce a smaller vasoconstriction compared with the natural Orpotrin, indicating that besides the *N*-terminal, the positive charge and the Pro residue located at the center of the amino acid chain is crucial for this vasoconstriction effect. Importantly, the suggestions made with bioactive peptides were based on the molecular modeling and dynamics of peptides, the presence of key amino acids and shared activity in microcirculation characterized by intravital microscopy [47,54]. The muscle microcirculation provides an opportunity to investigate the vasoactive properties of a compound, *in vivo*, in a relatively safe manner because of the small doses that are administered. However, further studies are required to determine which Orpotrin mechanisms and structures are required for this role as well the vasoactivity in other vascular beds.

Acknowledgment

Supported by funds provided by FAPESP and CNPq.

Supporting information

Supporting information may be found in the online version of this article.

References

1 Hodgson WC, Wickramaratna JC. Snake venoms and their toxins: an Australian perspective. *Toxicon* 2006; **48**: 931–940.
2 Joseph R, Pahari S, Hodgson WC, Kini RM. Hypotensive agents from snake venoms. *Curr. Drug. Targets Cardiovasc. Haematol. Disord.* 2004; **4**: 437–459.
3 Rasmussen H, Craig L. The isolation of arginine vasotocin from fish pituitary glands. *Endocrinology* 1961; **68**: 1051–1055.
4 Takenaka Y. On insulin from fish, especially mackerel and tunny. *Prod. Pharm.* 1962; **17**: 421–423.
5 Uzzell T, Stolzenberg ED, Shinnar AE, Zasloff M. Hagfish intestinal antimicrobial peptides are ancient cathelicidins. *Peptides* 2003; **24**: 1655–1667.
6 Pan CY, Chen JY, Cheng YS, Chen CY, Ni IH, Sheen JF, Pan YL, Kuo CM. Gene expression and localization of the epinecidin-1 antimicrobial peptide in the grouper (*Epinephelus coioides*), and its role in protecting fish against pathogenic infection. *DNA Cell. Biol.* 2007; **26**: 403–413.
7 Park CB, Lee JH, Park IY, Kim MS, Kim SC. A novel antimicrobial peptide from the loach *Misgurnus anguillicaudatus*. *FEBS Lett.* 1997; **411**: 173–178.
8 Oren Z, Shai Y. A class of highly potent antimicrobial peptides derived from pardaxin, a pore-forming peptide from the Moses sole fish *Pardachirus mamoratus*. *Eur. J. Biochem.* 1996; **237**: 304–310.
9 Silphaduang U, Noga EJ. Peptide antibiotics in mast cells of fish. *Nature* 2001; **414**: 268–269.
10 Shai Y, Fox J, Caratsch C, Shih YL, Edwards C, Lazarovici P. Sequencing and synthesis of pardaxin, a polypeptide from the Red Sea Moses sole with ionophore activity. *FEBS Lett.* 1988; **242**: 161–166.
11 Thompson SA, Tachibana K, Nakanishi K, Kubota I. Melittin-like peptides from the shark-Repelling defense secretion of the sole *Pardachirus pavoninus*. *Science* 1986; **233**: 341–343.
12 Bao B, Peatman E, Li P, He C, Liu Z. Catfish hepcidin gene is expressed in a wide range of tissues and exhibits tissue-specific upregulation after bacterial infection. *Dev. Comp. Immunol.* 2005; **29**: 939–950.
13 Kaiya H, Kodama S, Ishiguro K, Matsuda K, Uchiyama M, Miyazato M, Kangawa K. Ghrelin-like peptide with fatty acid modification and O-glycosylation in the red stingray, *Dasyatis akajei*. *BMC. Biochem.* 2009; **10**: 30.
14 Conceição K, Konno K, Melo RL, Marques EE, Hiruma-Lima CA, Lima C, Richardson M, Pimenta DC, Lopes-Ferreira M. Orpotrin: a novel vasoconstrictor peptide from the venom of the Brazilian stingray *Potamotrygon gr. orbignyi*. *Peptides* 2006; **27**: 3039–3046.
15 Conceição K, Santos JM, Bruni FM, Klitzke CF, Marques EE, Borges MH, Melo RL, Fernandez JH, Lopes-Ferreira M. Characterization of a new bioactive peptide from *Potamotrygon gr. orbignyi* freshwater stingray venom. *Peptides* 2009; **3012**: 2191–2199.
16 Fruitier I, Garreau I, Lacroix A, Cupo A, Piot JM. Proteolytic degradation of hemoglobin by endogenous lysosomal proteases gives rise to bioactive peptides: hemorphins. *FEBS Lett.* 1999; **447**: 81–86.
17 Brown AG, Leite RS, Engler AJ, Discher DE, Strauss III JF. A hemoglobin fragment found in cervicovaginal fluid from women in labor potentiates the action of agents that promote contraction of smooth muscle cells. *Peptides* 2006; **27**: 1794–1800.
18 Cho JH, Park IY, Kim HS, Lee WT, Kim MS, Kim SC. Cathepsin D produces antimicrobial peptide parasin I from histone H2A in the skin mucosa of fish. *FASEB J.* 2002; **16**: 429–431.
19 Powell WA, Catranis CM, Maynard CA. Synthetic antimicrobial peptide design. *Mol. Plant. Microbe. Interact.* 1995; **8**: 792–794.
20 Brust A, Palant E, Croker DE, Colless B, Drinkwater R, Patterson B, Schroeder CI, Wilson D, Nielsen CK, Smith MT, Alewood D, Alewood PF, Lewis RJ. chi-Conopeptide pharmacophore development: toward a novel class of norepinephrine transporter inhibitor (Xen2174) for pain. *J. Med. Chem.* 2009; **52**: 6991–7002.
21 Quinton L, Girard E, Maiga A, Rekik M, Lluel P, Masuyer G, Larregola M, Marquer C, Ciolek J, Magnin T, Wagner R, Molgó J, Thai R, Fruchart-Gaillard C, Mourier G, Chamot-Rooke J, Ménez A, Palea S, Servent D, Gilles N. Isolation and pharmacological characterization of AdTx1, a natural peptide displaying specific insurmountable antagonism of the alpha-adrenoceptor. *Br. J. Pharmacol.* 2010; **159**: 316–325.
22 Gibbons GH. Endothelial function as a determinant of vascular function and structure: a new therapeutic target. *Am. J. Cardiol.* 1997; **79**: 3–8.
23 Bachetti T, Morbidelli L. Endothelial cells in culture: a model for studying vascular functions. *Pharmacol. Res.* 2000; **42**: 9–19.
24 Bennett MR, Boyle JJ. Apoptosis of vascular smooth muscle cells in atherosclerosis. *Atherosclerosis* 1998; **138**: 3–9.
25 Jankowski J, Tepel M, van der Giet M, Tente IM, Henning L, Junker R, Zidek W, Schlüter H. Identification and characterization of P1,P7 Di(adenosine-5′)- heptaphosphate from human platelets. *J. Biol. Chem.* 1999; **274**: 23926–23931.
26 Østerud B, Bjørklid E. Role of monocytes in atherogenesis. *Physiol. Rev.* 2003; **83**: 1069–1112.
27 Heitzer T, Schlinzig T, Krohn K, Meinertz T, Munzel T. Endothelial dysfunction, oxidative stress, and risk of cardiovascular events in patients with coronary artery disease. *Circulation* 2001; **104**: 2673–2678.
28 Quyyumi AA. Prognostic value of endothelial function. *Am. J. Cardiol.* 2003; **91**: 19–24.
29 Hadi HA, Carr CS, Al Suwaidi J. Endothelial dysfunction: cardiovascular risk factors, therapy, and outcome. *Vasc. Health Risk Manag.* 2005; **3**: 183–198.
30 Hughes EL, Gavins FN. Troubleshooting methods: using intravital microscopy in drug research. *J. Pharmacol. Toxicol. Methods* 2010; **61**: 102–112.
31 Stewart JJP. Optimization of parameters for semiempirical methods V: modification of NDDO approximations and application to 70 elements. *J. Mol. Model.* 2007; **13**: 1173–1213.

32 Lindahl E, Hess B, Van der Spoel D. GROMACS 3.0: a package for molecular simulation and trajectory analysis. *J. Mol. Model.* 2001; **7**: 306–317.
33 Oostenbrink C, Villa A, Mark AE, van Gunsteren WF. A biomolecular force field based on the free enthalpy of hydration and solvation: the GROMOS force-field parameter sets 53A5 and 53A6''. *J. Comput. Chem.* 2004; **25**: 1656–1676.
34 Essman U, Perela L, Berkowitz ML, Darden T, Lee H, Pedersen LG. A smooth particle mesh Ewald method. *J. Chem. Phys.* 1995; **103**: 8577–8592.
35 Atherton E, and Sheppard RC. *Solid Phase Peptide Synthesis – A Practical Approach*. IRL Press: Oxford, 1989.
36 Baez S. An open cremaster muscle preparation for the study of blood vessels by in vivo microscopy. *Microvasc. Res.* 1973; **5**: 384–396.
37 Lomonte B, Lundgren J, Johansson B, Bagge U. The dynamics of local tissue damage induced by Bothrops asper snake venom and myotoxin II on the mouse cremaster muscle: an intravital and electron microscopic study. *Toxicon* 1994; **32**: 41–55.
38 Brubaker G, Peng DQ, Somerlot B, Abdollahian DJ, Smith JD. Apolipoprotein A-I lysine modification: effects on helical content, lipid binding and cholesterol acceptor activity. *Biochim. Biophys. Acta* 2006; **1761**: 64–72.
39 Koba H, Okuda K, Watanabe H, Tagami J, Senpuku H. Role of lysine in interaction between surface protein peptides of *Streptococcus gordonii* and agglutinin peptide. *Oral. Microbiol. Immun.* 2009; **24**: 162–169.
40 Davies JK, Hagan RM, Wilton DC. Effect of charge reversal mutations on the ligand and membrane-binding properties of liver fatty acid-binding protein. *J. Biol. Chem.* 2002; **277**: 48395–48402.
41 Labarrère P, Chatenet D, Leprince J, Marionneau C, Loirand G, Tonon MC, Dubessy C, Scalbert E, Pfeiffer B, Renard P, Calas B, Pacaud P, Vaudry H. Structure-activity relationships of human urotensin II and related analogues on rat aortic ring contraction. *J. Enzyme Inhib. Med. Chem.* 2003; **18**: 77–88.
42 Frare E, de Laureto PP, Scaramella E, Tonello F, Marin O, Deana R, Fontana A. Chemical synthesis of the RGD-protein decorsin: Pro→Ala replacement reduces protein thermostability. *Protein Eng. Des. Sel.* 2005; **18**: 487–495.
43 Crespo MD, Platt GW, Bofill R, Searle MS. Context-dependent effects of proline residues on the stability and folding pathway of ubiquitin. *Eur. J. Biochem.* 2004; **271**: 4474–4484.
44 Castanho MA, Fernandes MX. Lipid membrane-induced optimization for ligand-receptor docking: recent tools and insights for the ''membrane catalysis'' model. *Eur. Biophys. J.* 2006; **35**: 92–103.
45 Miller GJ, Ball EH. Conformational change in the vinculin C-terminal depends on a critical histidine residue (His-906). *J. Biol. Chem.* 2001; **276**: 28829–28834.
46 Wiebe CA, Dibattista ER, Fliegel L. Functional role of polar amino acid residues in Na+/H+ exchangers. *Biochem. J.* 2001; **357**: 1–10.
47 Friesenecker BE, Tsai AG, Martini J, Ulmer H, Wenzel V, Hasibeder WR, Intaglietta M, Dunser MW. Arteriolar vasoconstrictive response: comparing the effects of arginine vasopressin and norepinephrine. *Crit. Care.* 2006; **10**: R75.
48 Duling BR. Resistance arteries. In *Structure and Function*, Mulvany MJ, Aalkjaer C, Heagerty AM, Nyborg NBC, Strandgraard S (eds). Elsevier: Oxford, 1991; 3–9.
49 Cotte N, Balestre MN, Aumelas A, Mahe E, Phalipou S, Morin D, Hibert M, Manning M, Durroux T, Barberis C, Mouillac B. Conserved aromatic residues in the transmembrane region VI of the V1a vasopressin receptor differentiate agonist vs. antagonist ligand binding. *Eur. J. Biochem.* 2000; **267**: 4253–4263.
50 Cotte N, Balestre MN, Phalipou S, Hibert M, Manning M, Barberis C, Mouillac B. Identification of residues responsible for the selective binding of peptide antagonists and agonists in the V2 vasopressin receptor. *J. Biol. Chem.* 1998; **273**: 29462–29468.
51 Hausmann H, Richters A, Kreienkamp HJ, Meyerhof W, Mattes H, Lederis K, Zwiers H, Richter D. Mutational analysis and molecular modeling of the nonapeptide hormone binding domains of the [Arg8] vasotocin receptor. *Proc. Natl. Acad. Sci. U.S.A.* 1996; **93**: 6907–6912.
52 Mouillac B, Chini B, Balestre MN, Elands J, Trumpp-Kallmeyer S, Hoflack J, Hibert M, Jard S, Barberis C. The binding site of neuropeptide vasopressin V1a receptor. Evidence for a major localization within transmembrane regions. *J. Biol. Chem.* 1995; **270**: 25771–25777.
53 Rodrigo J, Pena A, Murat B, Trueba M, Durroux T, Guillon G, Rognan D. Mapping the binding site of arginine vasopressin to V1a and V1b vasopressin receptors. *Mol. Endocrinol.* 2007; **21**: 512–523.
54 McMahon PJ, Proctor KG. Vasopressin attenuates TNF-mediated inflammation in the rat cremaster microcirculation. *J. Trauma* 2009; **67**: 461–473.

